Trends in characterization and analysis of TKA implants for 3D printing

R. Dasharath[1], *Yeole Shivraj* Narayana[1]*, *Kode Jaya* Prakash[1], *and Narendra* Pothula[1]

[1]Department of Mechanical Engineering, VNR Vignana Jyothi Institute of Engineering & Technology, Hyderabad, Telangana, India

Abstract. In almost every country, knee joint problems are common among humans. As per American Academy of Orthopedic Surgeons, it is estimated that 3.5 million individuals in the world will undergo knee replacement surgery by 2030. People with advanced rheumatoid arthritis, or long-standing osteoarthritis are usually affected by this deformity due to changes in lifestyle. These conditions mainly affect middle-aged and elderly individuals with osteoarthritis or severe knee injuries. These problems can be overcome with the help of total knee implants by undergoing surgical procedures for providing relaxation & comfort to the knee joint. These procedures are also known as total knee arthroplasty (TKA). TKA is an ancient surgical process employed for treating intracapsular knee joint arthritis. It is promising technique greatly augmenting a patient's standard of life. The main components of TKA are femoral and tibial components, spacer, and patellar components respectively. Materials often used in these components include titanium, Ti6Al4V, cobalt-chromium alloys, polyethylene and bio compatible materials. 3D printing of TKA implants is a recent avenue being explored by researchers in an attempt to develop a better replacement for the conventional implants for providing comfort to the patients. This paper presents thorough assessment of research trends in mechanical characterization and finite element analysis of knee joint prosthetics, especially TKA implants for 3D printing.

1. Introduction to Total Knee Replacement

As a cost-effective and effective treatment for end-stage knee arthritis, knee replacement became widespread in the 1970s and 1980s [1]. Osteoarthritis (OA) has been the prime source of disability in the US and worldwide [2]. Approximately 25% of patients who undergo TKA for knee osteoarthritis are dissatisfied with the outcome of their operation [3]. By repairing the knee joint surface, osteoarthritis can develop, which causes the breakdown of the cartilage and meniscus, resulting in the femur and tibia bones rubbing against each other, resulting in extreme pain and discomfort in the knee when replacing the knee joint with implants [7]. In addition to being safe, custom-designed component of the femoral implant will last much longer for a patient with a more active lifestyle [4].

*Corresponding author: shivrajyeole@vnrvjiet.in

1.1. Anatomy of knee

Knee joint, a major joint in human body, involves extremely complex kinematics involved in the knee. Because of thesurrounding ligament structure, it has great stability despite its significant mobility. In addition to bearing weight, theknee also provides motion to the body. Ligaments, meniscus, and tibia and femur bones make up the hinge joint. Theknee joint is illustrated in Fig. 1 [5]. Two bones make up the knee: the femur and the tibia, which connect the femur (thigh bone) to the tibia (shin bone). Besides the tibia, the patella and fibula are also part of the knee joint [7]. An articulation between a femur and patella is known as femoropatellar articulation. Femorotibial articulation refers to the connection between femur and tibia. Anatomically, femurs have two articular structures called lateral and medial condyles. There is a slight difference in cross-sectional size between the lateral and medial condyles, but the former condyle is constant. When flexion occurs, the femoral and tibial condyles are able to slide and roll together [16].

Among bones, there are femurs, tibias, and patellas. In order to maintain the desired position of the knee bone, the ligament plays an important role.

• In the knee, cartilage is divided into two types: cartilage meniscus and articular cartilage.

• In the knee, the meniscus absorbs shocks so that the bones of the knee can move freely without friction. Balance, stability, and motion of the leg are all aided by the meniscus.

• Between the femur, tibia, and patella, there is a thin layer of cartilage called articular cartilage, which is thin and shiny.

• Soft tissues, such as tendons, connect bones and muscles to provide stability to joints [2].

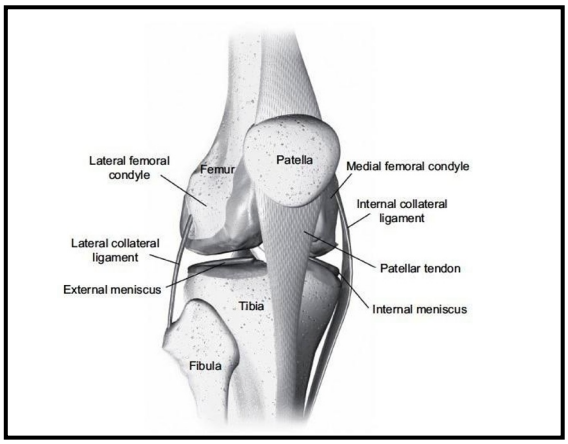

Figure 1. Anatomy of knee [5].

1.2. Components of Total Knee Replacement

The most traditional and effective surgical approach for treating intracapsular knee joint disease is total knee arthroplasty (TKA), which has substantial positive impact on patients quality of life. Postoperative infections are still among the most severe and difficult consequences following joint replacement, with a frequency of 0.66–30% and a reported case rate of 20.3% needing revision surgery [6]. The components of TKA are femoral, tibial, spacer, patellar as shown in Fig. 2 [7].

- Femoral component: The femoral condyle is a prosthetic implant that is used to replace the end of the femur bone. During motion of the knee, patella moves smoothly against the bone as the implant arches about the femur end.
- Spacer: Spacer, along with tibial component, acts as replacement to the top surface of the tibia. It helps in gliding the femur. Polymers are commonly used as spacers.
- Tibial tray: It is the flat platform holding the spacer. The components have been designed so the metal articulates smoothly with the plastic, which results in minimal wear and tear.
- Patellar: It is contained in a dome-shaped piece of polymer material that matches the patella's form and slides in the femur's groove.

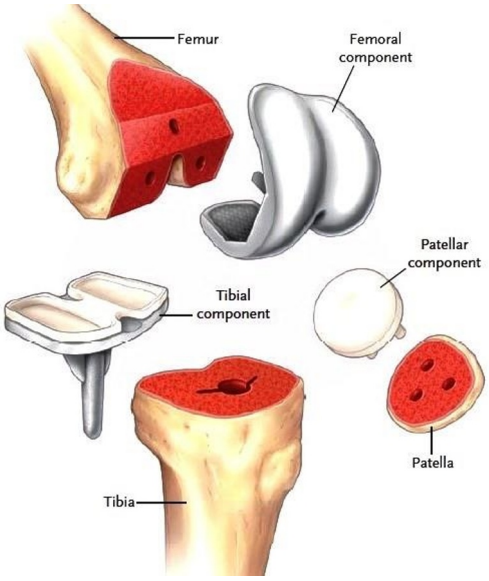

Figure 2. Components of Total Knee Arthroplasty [7].

1.3 Causes for Total Knee Arthroplasty implants

A TKA is usually implement when the cartilage is damaged, the joint is deformed, and worn cartilaginous bearing surfaces need to be replaced with artificial bearings [8]. The objective of arthroplasty is not to treat disease, but rather to solve a biological problem mechanically. There may be no other option for patients suffering from severe joint damage than arthroplasty [9]. It has been found that obese patients with TKA have greater functional improvements than those with a normal body mass index [10-11]. The functional outcomes after TKA can, however, be improved by focusing on treating excess weight related issues of patient [12]. It is reported that in 31% cases TKA resulted in loss of weight and improved BMI as well as functional outcomes [13]. Around 781 revision TKAs have been carried out. Loosening (39.5%), infection (27.3%), instability (7.5%), periprosthetic fracture (4.7%), and arthrofibrosis (4.5%) were a few of the frequent failure reasons. Prime reasons for recurrent TKA failures are reported as aseptic loosening, infection, instability, periprosthetic fracture, and arthrofibrosis. Fig. 3 depicts summary of failures and their causes in TKA.

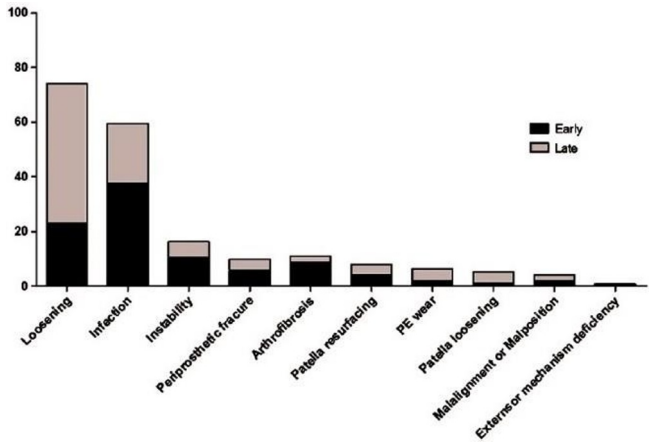

Figure 3. Subgroups of patients with early, late, and total failure for each failure cause, according to the percentage of patients [14].

2. Screening Techniques of Osteoarthritis

Degeneration of ligaments in patients can be assessed through different methods. some of them are given below.

- **Radiography (X-ray)**

OA screening is primarily carried out using X-rays of the joint space width (JSW) as they are less invasive and may be repeated if need be. However, this technique lacks accuracy for instantaneous tests, as the changes in ligaments need to be recorded using X-rays for 2-3 years [18].

- **Magnetic Resonance Imaging (MRI)**

Patients with knee arthroplasty implants can benefit from complete imaging evaluation and monitoring using MR imaging with tailored conventional and advanced pulse sequences. To compensate for the effects of changes in the static magnetic field caused by large differences in the magnetic susceptibility constant between the metallic implant components and the surrounding tissue, MRI of metallic implants need altered and progressive pulse sequences [35].

- **Computed Tomography (CT Scan)**

MRI and CT scans may both be used to obtain 3D data. The final models will invariably deviate from the real form and size of the bone due to the numerous measurement phases and manufacturing procedures. CT scan- generated bone models have been found to be more accurate, with smoother exterior surface boundaries and lessdistorting artefact than MRI-generated models [17].

2.1. Generation of Point Cloud Data

A fully automated thresholding approach is utilized for reliable and accurate bone segmentation in CT images. The photos are first segmented to separate them into bone and non-bone groups. The borders of bones are detected in the following iterative process by applying image processing techniques such as edge detection [19]. Medical image processing software converts the obtained MDCT pictures, also known as DICOM images, into three-dimensional CAD data. For processing CT slice pictures, segmentation of the region of interest (ROI) of 3D CAD data and image binarization are carried out [20]. Fig. 4 summarizes the stages involved in generation of point cloud data.

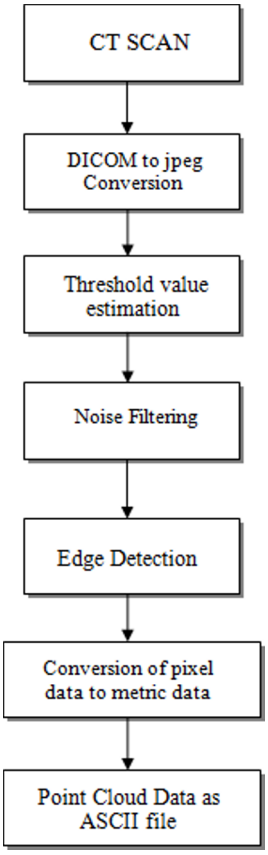

Figure 4. Methodology for generation of point cloud data [19].

3. 3D Printed TKA

According to reports, upto 19% of patients are dissatisfied after total knee replacement (TKR). One reason to which it can be attributed is minor misalignment of the tibial component in the coronal plane which leads to loosening. Instrumentation for knee replacement is patient-specific. It's intended to educate orthopaedic doctors on the terminology used in this field and to compare the benefits and drawbacks of 3D printing processes [17]. Customized implants aim to go above the limitations of the pre-made prosthesis by being made for the unique anatomy of the patient. Due to advancements in 3D imaging software and 3D printing, it is now possible to create and use medical devices that are geared for individual patients [3]. The two most popular techniques for creating titanium implants are DMLS and EBM. In one study involving TKA with 3D printing assistance, better short-term clinical effects than traditional TKA notably increased surgical efficiency and post-operative force line accuracy and enhanced post- operative knee function [15-16]. In another study, SolidWorks software was used to create the anatomical CAD model, and Ansys was used to analyse biomechanical behaviour of the knee joint [21]. A comprehensive 3D model was constructed using CREO software. Under various loading situations and stress distributions, the knee prosthesis' FEA analysis was assessed [22].

3.1. 3D printed materials for TKA

Typically, spacer materials consist of ultra-high molecular weight polyethylene (UHMWPE) or poly carbonate-ISO (PC-ISO). The suggested material for spacer is PC-ISO. PC-ISO is an industrial thermoplastic that may be treated using gamma radiation or ethylene oxide and is biocompatible in its unprocessed condition. By cementing the femoral component and tibial tray to the bone, polymethylmethacrylate (PMMA) can be used to fix the components [23]. FDM can produce components with exceptional thermal and chemical resistance as well as great strength to weight ratios since 3D printing technology utilises ABS, PC-ISO polycarbonate, and ULTEM9085 materials [24]. DMLS and EBM are the methods widely used for making implants [25]. Highly cross-linked polyethylene, also known as second-generation polyethylene, was first introduced around 20 years ago and has proved to be successful in reducing polyethylene wear, decreasing aseptic loosening and revision as a result [26]. Titanium alloys are found to be the best suited materials for making implants as titanium is corrosion resistant to bodily fluids and the oxide layer that forms on top of it prevents it from further corrosion. In TKR reshaping of femur bone and tibia bone, femur component (Cobalt-Chromium (CoCr) alloy or titanium) is fixed to thigh bone. Tibia tray made up of titanium is locked to shine bone. A spacer (plastic) made of polyethylene is placed in between these two bones [1]. A femoral spacer, a tibial spacer, and a canal rod make up the unique spacer set. Medical-grade UHMWPE with confirmed biocompatibility is used to make the spacers [27]. The selective laser melting technique was used to create the CoCr femoral component utilising 3D printing. The components of the tibia and the tibial insert were machined from Ti6Al4V and common polyethylene, respectively [28].

4. Mechanical characterization

In order to perform mechanical characterization studies on these TKR implants, test specimens are designed and tested as per corresponding ASTM standards of biocompatible material. ASTM D638 utilised for tensile testing [29] and ASTM D7774 for fatigue testing [30].

4.1. Tensile testing

Fig. 5. (a) and (b) illustrates plots of stress vs strain and experimental tensile modulus and tensile strength findings respectively, along with reference data from PC-ISO manufacturer. Tensile strength of 57 MPa and tensile modulus of 2000 MPa as indicated in the PC-ISO datasheet, are represented by the red and blue dotted lines, respectively [29]. Brittle failure occurs when two neighbouring layers separate as a result of fracture in the Z-direction. Results show that the junctions between layers have lower resistance than the filament polymer itself. Maximum achievable tensile modulus of 13.48 to 20.6 GPa and shear shear modulus 4.52 to 6.23 GPa of PC-ISO is approximately 10% of the known cortical bone stiffness [31]. Values obtained for tensile strengths are nearer between 42% and 77% of the reported strength, which ranges from 80 to 150 MPa, however variability is wider [32].

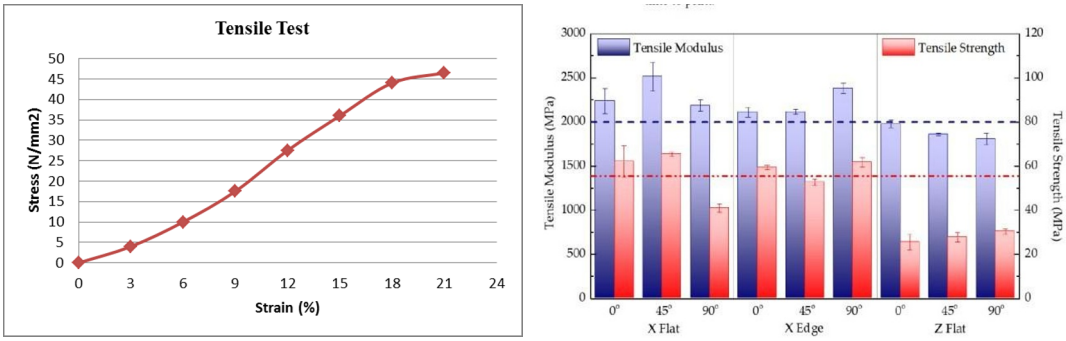

Figure 5. (a) Stress v/s Strain plot for the PC-ISO tensile specimen [23]; (b) Comparison of modulus and strength [29].

4.2 Fatigue and impact testing

Fatigue strength is affected by raster angle and print orientation which is mostly determined by the print arrangement. With the exception of X-Flat 90° and Z-Flat 45°, the limited life (10,000 cycles) is attained at lower loading percentages. Higher load percentages have more noticeable changes, thus using them is not advised unless higher safety considerations are taken into account. Fig. 6 (a) and (b) exhibit effect of SN curves at different raster angle orientation for the X-Flat test configuration [34].

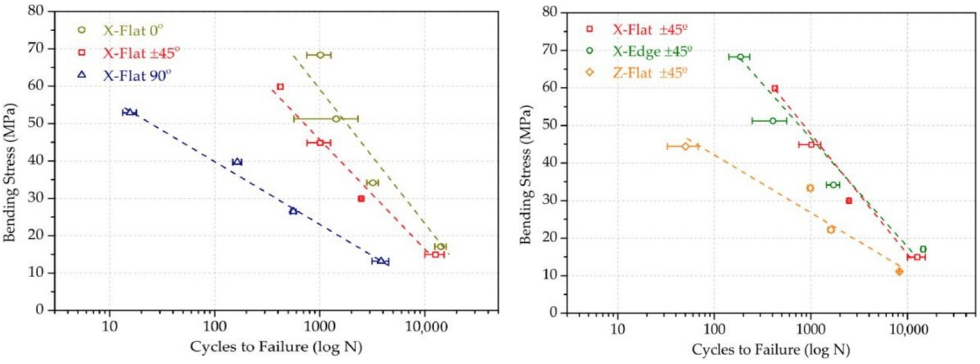

Figure 6. SN curves of fatigue performance on biocompatible materials. (a) X-Flat test raster angle effects; (b) Effect of the orientation sample for raster angle with ±45° [34].

The parameters for the fatigue tests were determined as per ASTMF1800 (Fig. 7A). A commercial metallic femoral condyle (U2 knee, United Orthopedic Corporation, Taiwan) was employed in the study. One side of the tibial condyles was fastened to the bottom fixture and on other side, cantilever beam load was applied [29]. 5 Hz frequency was chosen for the test as per the guidelines. In order to determine the stability of test specimens in cyclic loading, peak and valley displacements were measured as shown Fig. 7 [27].

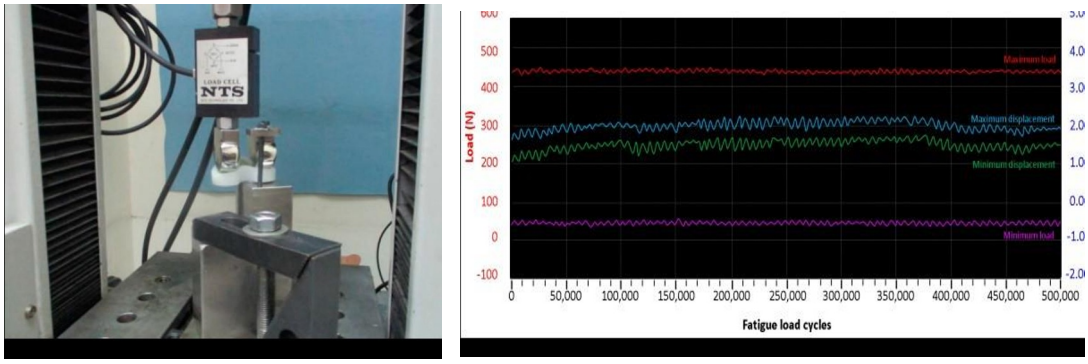

(a) (b)

Figure 7. (a) Fatigue test on tibial spacer; (b) Load and displacement data that have been recorded [27].

4.2. Wear test

Medical-grade UHMWPE was used for the wear test in accordance with ISO 14243-1 guidelines. Articulating cycles were reduced down to 5 × 105 cycles. The remaining two sets of femoral/tibial spacers were manufactured as test controls. A total of six femoral/tibial spacer sets were employed for wear test. Specimens were pre-soaked without application of wear loads [27]. Using a knee-wear simulator and the input waveforms mentioned, wear testing on polyethylene (PE) material was done over a period of 5 million cycles at a frequency of one hertz (Hz). Results depicted in Fig. 8 showed substantial resemblance similarity to wear contours of computed optimal model [28].

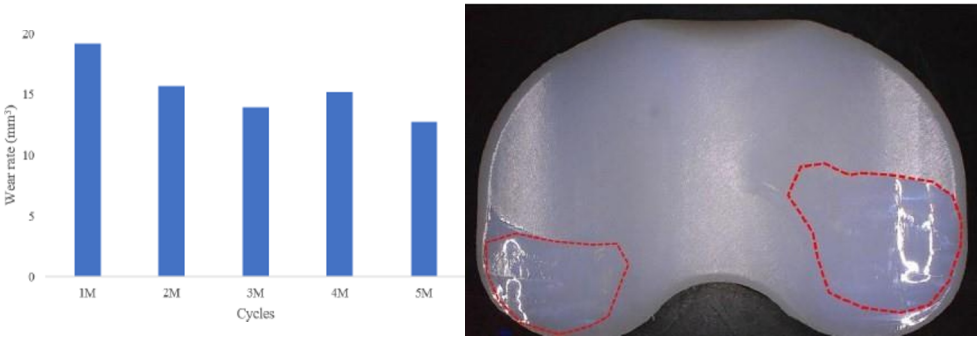

(a) (b)

Figure 8. Experimental wear rates on UHMWPE material: (a) Optimal model wear rate after 1Million cycles; b) wear pattern after 5Million cycles [28].

5. FEA on TKA

5.1. Computational wear analysis

Fig. 9 shows initial and optimal model wear curves after 5 million cycles. In the original model, the wear contour depicted shallow wear scar on lateral side and a deeper wear region at middle of the medical side.

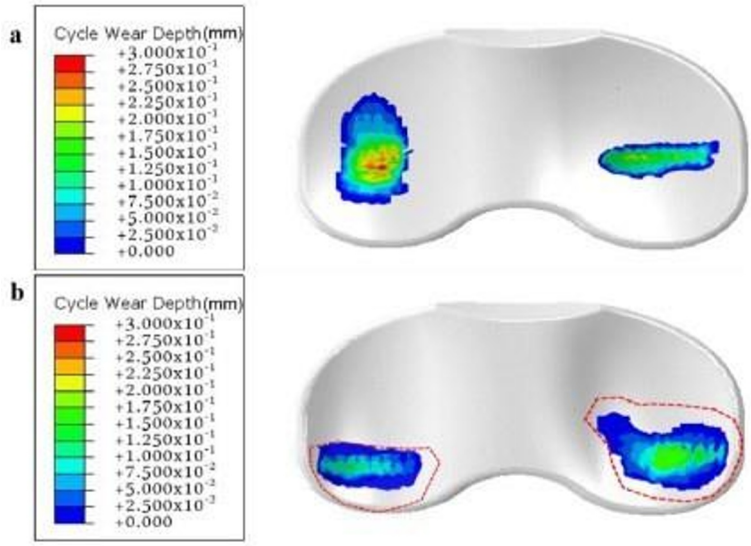

Figure 9. Computational wear models after 5 million cycles: (a) Initial; (b) Optimal [28].

5.2. Tibial insert

The PC-ISO tibial spacer insert's strength and durability under static stress were predicted and validated using FEM analysis. Analysis was done on the deformation and stress distribution. In order to put the spacer component on the tibial tray, the bottom surface was secured in all DOF. Over the top surface, uniform pressures of estimated magnitudes were applied in accordance with spacer size. Regardless of the loading and size circumstances, PC-ISO delivers a very low deformation rate, it may be said. As a result, the knee implant's spacer insert can endure both static and dynamic stress conditions [23].

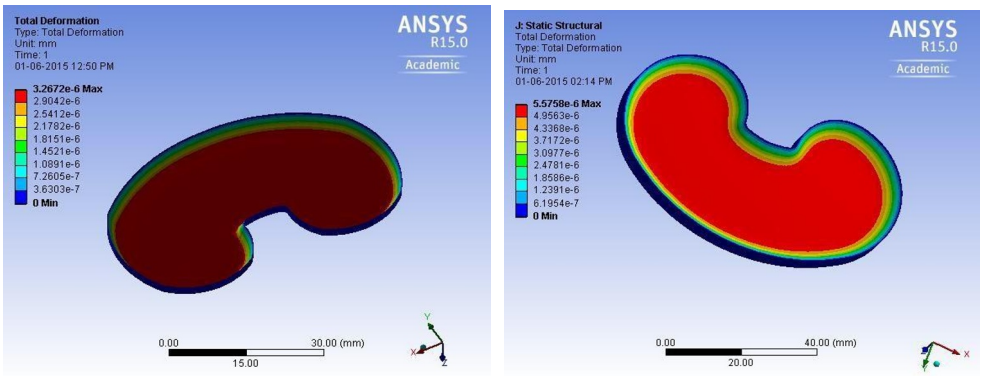

(a) (b)

Figure 11. Spacer deformation in two sizes: (a) 2 mm thick; (b) 6 mm thick [23].

5.3. Femoral component

Fig. 12 presents a study examining stress distribution in Titanium Ti6Al4V alloy implant. Maximum tension is represented by red colour, whereas normal stress is represented by the green colour. Stresses in the conventional implant were seen to be highly concentrated along sharp edges whereas they were uniformly distributed in custom implant. Maximum stress

produced by the custom-designed implant was substantially lower. In the centre position instance for the custom implant with smooth surface design (lower picture), Average stresses in custom-designed implant with smooth surface were noted to be 6.687 MPa, whereas in conventional implant were 16 MPa. [4].

(a) (b) (c)

Figure 12. (a) Load and reaction force; (b) Distribution of stress in the conventional implant;

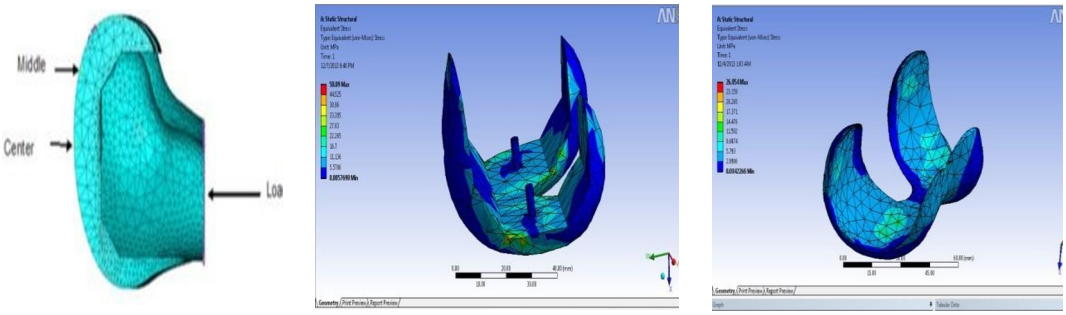

(c) Distribution of stress in custom implant [4].

5.4. Tibial component (tray)

Fig. 13 shows distribution of contact pressure on tibial insert in a fluid and bouncy gait. Maximum contact pressure is observed in bouncy gait at the second peak contact force, while lowest stresses are seen at smooth gait patterns A and B. Increased contact forces result from the sudden variations in joint flexion and axial forces that occur in bouncy gait. As a result, the increased tibiofemoral contact forces result in increased contact pressures. On the other hand, it is anticipated that smooth walking will reduce the pressure distribution at the knee joint. The contact pressures that were detected in patient's various gait patterns are found to be in good range [33].

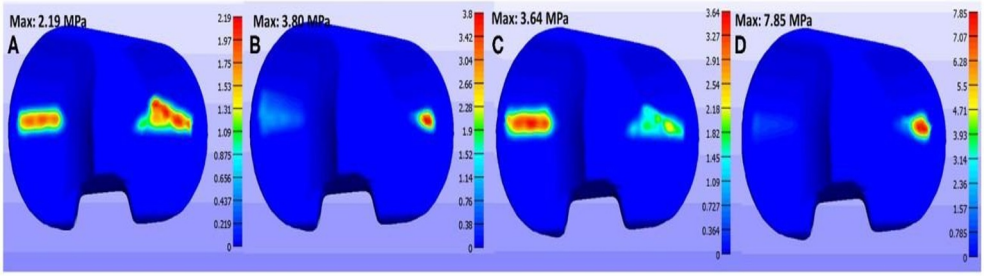

Figure 13. Tibial insert contact pressure at: (a) smooth gait during first axial peak force; (b) smooth gait during second axial peak force; (c) bouncy gait during first peak force; (d) bouncy gait during second axial peak force [33].

6. Conclusion

This study provides an overview of 3D printed total knee arthroplasty, that have been constructed as part of research, individual projects, and worldwide community projects. For knee implants, biocompatible components like Cobalt- Chromium (CoCr) alloy, titanium, and UHMWPE materials were mostly used as articulating components. A CT scan provides accurate patient-specific data in DICOM format compared to X-ray and MRI, which are used for creating 3D models and TKA components. In comparison with conventional TKR, 3D printed TKR offer various benefits. Materials are generally cheap to buy, however,

development includes designing, assembling, and fitting the TKR according to the patient's requirements as well. With 3D printing, prostheses can be customized, such as specifications and colour, shape and size, without having to change the standard parts that were machined by conventional methods.

References

1. Carr, A. J., Robertsson, O., Graves, S., Price, A. J., Arden, N. K., Judge, A., & Beard, D. J. Knee replacement. *The Lancet*, *379*(9823), 1331-1340, (2012). DOI: https://doi.org/10.1016/S0140-6736(11)60752-6.
2. Lespasio, M. J., Piuzzi, N. S., Husni, M. E., Muschler, G. F., Guarino, A. J., & Mont, M. A. Knee osteoarthritis: a primer. *The Permanente Journal*, *21*, (2017). DOI: https://doi.org/10.7812/TPP/16-183.
3. Ghidotti, A., Vitali, A., Regazzoni, D., & Rizzi, C. An Investigation of Innovative 3D Modelling Procedures for Patient-specific Total Knee Arthroplasty, (2022). DOI: https://doi.org/10.14733/cadaps.2022.306-319.
4. Alyazji, Q., Topukçu, Z., & Kassem, Y. Custom Design of Knee Joint Prosthesis By Using ComputerizedTomography (CT) Images and 3D Modelling. *Int. J. Biomed. Eng. Sci*, *1*, 1-9, (2014).
5. Castiello,E., & Affatato, S. Istituto OrtopedicoRizzoli, Bologna, Italy, (2015).DOI: http://dx.doi.org/10.1533/9781782420385.2.109.
6. Varacallo, M., Luo, T. D., & Johanson, N. A. Total knee arthroplasty techniques. In *StatPearls [Internet]*.StatPearls Publishing, (2022).
7. Leopold, S. S. Minimally invasive total knee arthroplasty for osteoarthritis. *New England Journal ofMedicine*, ***360***(17), 1749-1758, (2009). DOI: 10.1056/NEJMct0806027.
8. Garampalli, A., Patil, A., & Quadri, M. Our experience of total knee arthroplasty in rural Karnataka region. *International Journal of Orthopaedics*, ***6***(1),1082-1088, (2020). DOI: https://doi.org/10.22271/ortho.2020.v6.i1n.1966.
9. Tande, A. J., & Patel, R. Prosthetic joint infection. *Clinical microbiology reviews*, *27*(2), 302-345, (2014). DOI: https://doi.org/10.1128/CMR.00111-13.
10. Parratte, S., Pesenti, S., & Argenson, J. N. Obesity in orthopedics and trauma surgery. *Orthopaedics & Traumatology: Surgery & Research*, *100*(1), S91-S97, (2014). DOI: https://doi.org/10.1016/j.otsr.2013.11.003.
11. Bin Abd Razak, H. R., Chong, H. C., & Tan, A. H. C. Obesity does not imply poor outcomes in Asians after total knee arthroplasty. *Clinical Orthopaedics and Related Research®*, *471*(6), 1957-1963, (2013).
12. Si, H. B., Zeng, Y., Shen, B., Yang, J., Zhou, Z. K., Kang, P. D., & Pei, F. X. The influence of body mass index on the outcomes of primary total knee arthroplasty. *Knee Surgery, Sports Traumatology, Arthroscopy*, *23*(6), 1824-1832, (2015).
13. Ast, M. P., Abdel, M. P., Lee, Y. Y., Lyman, S., Ruel, A. V., & Westrich, G. H. Weight changes after total hip or knee arthroplasty: prevalence, predictors, and effects on outcomes. *JBJS*, *97*(11), 911- 919, (2015). DOI: 10.2106/JBJS.N.00232.
14. Sharkey, P. F., Lichstein, P. M., Shen, C., Tokarski, A. T., & Parvizi, J. Why are total knee arthroplasties failing today—has anything changed after 10 years?. *The Journal of arthroplasty*, *29*(9), 1774-1778, (2014). DOI: https://doi.org/10.1016/j.arth.2013.07.024.
15. Zhang, G., Li, J., Zhou, X., Zhou, Y., & Wang, A. Optimal Design and Processing Technology of 3D Printed Tibial Implants. *Coatings*, *12*(5), 561, (2022). DOI: https://doi.org/10.3390/coatings12050561.

16. Bautista, A. I. A Finite Element Analysis of Tibial Stem Geometry for Total Knee Replacements. (2015). DOI: https://doi.org/10.15368/theses.2015.111.
17. Krishnan, S. P., Dawood, A., Richards, R., Henckel, J., & Hart, A. J. A review of rapid prototyped surgicalguides for patient-specific total knee replacement. *The Journal of bone and joint surgery. British volume*, ***94***(11), 1457-1461, (2012). DOI: https://doi.org/10.1302/0301-620X.94B11.29350.
18. Khalid, H., Hussain, M., Al Ghamdi, M. A., Khalid, T., Khalid, K., Khan, M. A., ... & Ahmed, A. A comparative systematic literature review on knee bone reports from MRI, x-rays and ct scans using deep learning andmachine learning methodologies. *Diagnostics*, ***10***(8), 518, (2020). DOI: https://doi.org/10.3390/diagnostics10080518.
19. Chougule, V. N., Mulay, A. V., & Ahuja, B. B. (2013, December). Conversions of CT scan images into 3D pointcloud data for the development of 3D solid model using B-Rep scheme. In *Proceedings of the International Conference on Precision, Meso, Micro and Nano Engineering* (Vol. 2).(2013).
20. Narita, M., Takaki, T., Shibahara, T., Iwamoto, M., Yakushiji, T., & Kamio, T. Utilization of desktop 3D printer-fabricated "Cost-Effective" 3D models in orthognathic surgery. *Maxillofacial plastic and reconstructive surgery*, *42*(1), 1-7, (2020).
21. Kumar, V. J., Reddy, P. S., & Murthy, N. G. Modeling and biomechanical analysis of human kneejoint. *Int. J. Sci. Eng. Adv. Technol*, *2*, 246-252, (2014).
22. Kumbhalkar, M. A., Nawghare, U., Ghode, R., Deshmukh, Y., & Armarkar, B. Modeling and finite element analysis of knee prosthesis with and without implant. *Universal Journal of Computational Mathematics*, *1*(2),56-66, (2013). DOI: 10.13189/ujcmj.2013.010204.
23. Harish, S., & Devadath, V. R. Additive manufacturing and analysis of tibial insert in total knee replacement implant. *Int Res J Eng Technol*, *2*(04), 633-638, (2015).
24. Attarilar, S., Ebrahimi, M., Djavanroodi, F., Fu, Y., Wang, L., & Yang, J. 3D printing technologies in metallic implants: a thematic review on the techniques and procedures. *International Journal of Bioprinting*, *7*(1), (2021). DOI: https://doi.org/10.18063%2Fijb.v7i1.306
25. Boorla, R., & Prabeena, T. Fabrication of patient specific knee implant by fused deposition modeling. *Materials Today: Proceedings*, *18*, 3638-3642, (2019). DOI: https://doi.org/10.1016/j.matpr.2019.07.296.
26. Price, A. J., Alvand, A., Troelsen, A., Katz, J. N., Hooper, G., Gray, A., ... & Beard, D. Hip and kneereplacement 2 Knee replacement. *Lancet*, *392*, 1672-1682, (2018). DOI: https://doi.org/10.1016/S0140-6736(18)32344-4.
27. Chang, Y., Lee, M. S., Liau, J. J., Liu, Y. L., Chen, W. C., & Ueng, S. W. Polyethylene-based knee spacer for infection control: design concept and pre-clinical in vitro validations. *Polymers*, *12*(10), 2334, (2020). DOI: https://doi.org/10.3390/polym12102334.
28. Koh, Y. G., Jung, K. H., Hong, H. T., Kim, K. M., & Kang, K. T. Optimal design of patient-specific totalknee arthroplasty for improvement in wear performance. *Journal of Clinical Medicine*, ***8***(11), (2023). DOI: https://doi.org/10.3390/jcm8112023.
29. Kuehn, K. D., Ege, W., & Gopp, U. Acrylic bone cements: mechanical and physical properties. *Orthopedic Clinics*, *36*(1), 29-39, (2005). DOI: https://doi.org/10.1016/j.ocl.2004.06.011.
30. Mellman, I. S., Plutner, H., Steinman, R. M., Unkeless, J. C., & Cohn, Z. A.. Internalization and degradation of macrophage Fc receptors during receptor-mediated phagocytosis. *The Journal of cell biology*, *96*(3), 887-895(1983) DOI: https://doi.org/10.1083/jcb.96.3.887.
31. Sieving, A., Wu, B., Mayton, L., Nasser, S., & Wooley, P. H. Morphological characteristics

of total jointarthroplasty-derived ultra-high molecular weight polyethylene (UHMWPE) wear debris that provoke inflammation ina murine model of inflammation. *Journal of Biomedical Materials Research Part A: An Official Journal of The Societyfor Biomaterials, The Japanese Society for Biomaterials, and The Australian Society for Biomaterials and the KoreanSociety for Biomaterials*, *64*(3), 457-464, (2003). DOI: https://doi.org/10.1002/jbm.a.10368.

32. Elke, R., & Rieker, C. B. Estimating the osteolysis-free life of a total hip prosthesis depending on the linear wear rate and head size. *Proceedings of the Institution of Mechanical Engineers, Part H: Journal of Engineering in Medicine*, *232*(8), 753-758, (2018). DOI: https://doi.org/10.1177/0954411918784982.
33. Loi, I., Stanev, D., & Moustakas, K. Total knee replacement: subject-specific modeling, finite element analysis, and evaluation of dynamic activities. *Frontiers in Bioengineering and Biotechnology*, *9*, 648356, (2021).
34. Gómez-Gras, G., Abad, M. D., & Pérez, M. A. Mechanical performance of 3D-printed biocompatible polycarbonate for biomechanical applications. *Polymers*, *13*(21), 3669, (2021). DOI: https://doi.org/10.3389/fbioe.2021.648356.
35. Fritz, J., Lurie, B., & Potter, H. G. MR imaging of knee arthroplasty implants. *Radiographics*, *35*(5),1483-1501, (2015). DOI: https://doi.org/10.1148/rg.2015140216.